Adiabatic pseudospectral calculation of vibrational states of four atom molecules: Application to hydrogen peroxide

J. Antikainen, R. Friesner, and C. Leforestier

Citation: The Journal of Chemical Physics **102**, 1270 (1995); doi: 10.1063/1.468915
View online: http://dx.doi.org/10.1063/1.468915
View Table of Contents: http://scitation.aip.org/content/aip/journal/jcp/102/3?ver=pdfcov
Published by the AIP Publishing

Adiabatic pseudospectral calculation of vibrational states of four atom molecules: Application to hydrogen peroxide

J. Antikainen[a] and R. Friesner
Department of Chemistry, Columbia University, New York, New York 10027

C. Leforestier
Laboratoire de Chemie Théorique, UA 506, Université de Paris-Sud, 91405 Orsay, France

(Received 25 July 1994; accepted 12 October 1994)

We use our adiabatic pseudospectral method (APS) to calculate energy levels of the H_2O_2 molecule up to 5000 cm^{-1}. Reasonably high accuracy (a few wave numbers) is achieved for a fully six dimensional calculation in a few hours of CPU time on an IBM 580 workstation. This contrasts with previous calculations on the same system which required 50–100 times more computational effort for a similar level of accuracy. The method presented here is both general and robust, and will allow routine studies of six dimensional potential surfaces and the associated spectroscopy, while making calculations on still larger systems feasible. © *1995 American Institute of Physics.*

I. INTRODUCTION

The quantum mechanical calculation of accurate vibrational states and spectra for polyatomic molecules, given the potential energy surface, remains a major goal of computational chemical physics. The continued increase in the power of computational hardware coupled to improved algorithms has led to significant advances in this area over the past several years. In particular, the introduction of collocation[1] and DVR[2] methods, the use of iterative eigensolvers such as the Lanczos algorithm,[3] and the use of sequential adiabatic reduction[4–6] have all contributed to making three-dimensional problems routine and as many as six-dimensional problems accessible with workstation technology.

In a previous paper,[7] we presented a synthesis of collocation, adiabatic sequential reduction, and Lanczos methods which led to highly efficient calculation of eigenvalues and spectra for the highly excited states of the triatomic molecule HCN. In that paper, our comparison of standard collocation techniques with our new method, the adiabatic pseudospectral method (APS) indicated that as much as an order of magnitude improvement in performance could be obtained. While recent work by Bramley and Carrington finds a somewhat smaller advantage, which may be due to the details of the methodologies or in the different error analyses that were mandated in the two papers, the APS still emerges as the most efficient approach.

However, we expected that significantly more substantial advantages would be obtained for larger dimensional problems, where the adiabatic reduction is allowed to act over six, rather than three dimensions. In the present paper, we describe calculations on the H_2O_2 molecule, which has been identified by Bramley and Handy[8] as a particularly difficult case. We calculate the eigenvalues below 5000 cm^{-1} to an accuracy of a few wave numbers. It is our view that greater accuracy than this is irrelevant to practical applications because the potential energy functions are almost certainly not more accurate than 10–20 cm^{-1} for higher excited states, even if adjustment of parameters can produce eigenvalues in better agreement with experiment. Even if the potential energy surface could be made more accurate than this, it is difficult to see what the motivation would be in terms of understanding chemistry.

We are able to carry out our calculations for H_2O_2 in a few hours of workstation CPU time. In contrast, standard basis set methods require the diagonalization of 6000×6000 matrices, necessitating the use of supercomputers because of the demand for fast memory and massive amounts of CPU time.[8] The collocation calculations of Bramley and Carrington on this same molecule, while tractable on a workstation, required 100 h of single processor CPU time per symmetry block (200 h total) to achieve similar results.[9] While improvements in the collocation methodology are no doubt possible and a precise comparison is difficult because of accuracy issues, the performance of the APS algorithm for the present six dimensional case appears at present to be qualitatively superior to the alternatives.

The methodology for constructing an adiabatic basis and the associated pseudospectral operators presented below is completely general and can readily be applied to other six-dimensional (or larger) problems. For example, we should be able to examine the highly excited vibrational states of acetylene and make comparisons with the SEP spectra of Field and co-workers.[10] More generally, the present program should be quite useful in optimizing six dimensional potential surfaces. Lower resolution calculation of spectra can be carried out even more quickly and this will be valuable in the initial stages of potential fitting.

The paper is organized into five sections. In Sec. II, we define the Hamiltonian for H_2O_2 and discuss our representations of the kinetic and potential energy operators. Section III presents the adiabatic reduction procedure, the implementation of the matrix–vector product for the Hamiltonian in the reduced adiabatic representation, and the Lanczos iteration scheme, which together constitute the APS. Section IV describes results for H_2O_2 in computing the eigenstates below 5000 cm^{-1}, comparing to the results of Bramley *et al.*: we

[a]In partial fulfillment of the Ph.D. in the Department of Physics, Columbia University.

 0021-9606/95/102(3)/1270/10/$6.00

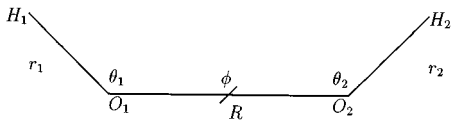

FIG. 1. The Jacobian coordinate system used in calculations. The torsion angle is labeled by ϕ, bending angles by θ_1 and θ_2, and stretches by R, r_1, and r_2.

also calculate a spectrum and examine its convergence as a function of the number of iterations. Finally, in the conclusion, Sec. V, we discuss future directions.

II. THE HAMILTONIAN

A. Representation of the H_2O_2 Hamiltonian in Jacobi coordinates

In Jacobi coordinates the four-atom Hamiltonian has a particularly simple form. In Fig. 1 Jacobi coordinates r_1, r_2, and R give the hydrogen–oxygen bond lengths and the oxygen–oxygen bond length, respectively. Bending angles H–O–O and O–O–H are given by θ_1 and θ_2. ϕ is the HO–OH torsion angle.

The $J=0$ Hamiltonian in Jacobi coordinates is given as[11]

$$H=V+T=^{\text{def}}V+\left(T1+T2+T3+\frac{1}{I_4}\,T4+\frac{1}{I_5}\,T5+\frac{1}{I_6}\,T6 +TC1+TC2+TC3+TC4\right), \tag{1}$$

where V is the electronic ground state potential energy surface V_g from Ref. 12 and consists of terms of the form

$$V_k=c_k\,\frac{\Delta r_1^{I1}\Delta r_2^{I2}\Delta\theta_1^{I3}\Delta\theta_2^{I4}\Delta R^{I5}\,\cos(I_6\phi)}{I_1!I_2!I_3!I_4!I_5!}. \tag{2}$$

The potential energy surface is expanded about the minimum point of the potential energy surface.

The kinetic energy terms are

$$T1+T2+T3=-\frac{1}{2}\,\frac{1}{\mu_{12}R^2}\,\frac{\partial}{\partial R}\,R^2\,\frac{\partial}{\partial R} -\frac{1}{2}\,\frac{1}{\mu_1 r_1^2}\,\frac{\partial}{\partial r_1}\,r_1^2\,\frac{\partial}{\partial r_1} -\frac{1}{2}\,\frac{1}{\mu_2 r_2^2}\,\frac{\partial}{\partial r_2}\,r_2^2\,\frac{\partial}{\partial r_2},$$

$$\frac{1}{I_4}\,T4=-\frac{1}{I_4(R,r_1)}\,\frac{1}{2}\,\frac{1}{\sin\theta_1}\,\frac{\partial}{\partial\theta_1}\sin\theta_1\,\frac{\partial}{\partial\theta_1},$$

$$\frac{1}{I_5}\,T5=-\frac{1}{I_5(R,r_2)}\,\frac{1}{2}\,\frac{1}{\sin\theta_2}\,\frac{\partial}{\partial\theta_2}\sin\theta_2\,\frac{\partial}{\partial\theta_2},$$

$$\frac{1}{I_6}\,T6=-\frac{1}{I_6(R,r_1,r_2,\theta_1,\theta_2)}\,\frac{1}{2}\,\frac{\partial^2}{\partial\phi^2},$$

$$TC1+TC2=\frac{1}{\mu_{12}R^2}\left(\cos\phi\,\frac{\partial^2}{\partial\theta_1\partial\theta_2} -\sin\phi\,\cot\theta_2\,\frac{\partial^2}{\partial\theta_1\partial\phi}\right),$$

$$TC3+TC4=\frac{1}{\mu_{12}R^2}\left[-\sin\phi\,\cot\theta_1\,\frac{\partial^2}{\partial\theta_2\partial\phi} +(1-\cot\theta_1\,\cot\theta_2\,\cos\phi)\,\frac{\partial^2}{\partial\phi^2}\right],$$

in which

$$\frac{1}{\mu_{12}}=\frac{2}{m_H+m_O},\quad \frac{1}{\mu_1}=\frac{1}{m_H}+\frac{1}{m_O},$$

$$\frac{1}{\mu_2}=\frac{1}{m_H}+\frac{1}{m_O},\quad \frac{1}{I_4(R,r_1)}=\frac{1}{\mu_{12}R^2}+\frac{1}{\mu_1 r_1^2},$$

$$\frac{1}{I_5(R,r_2)}=\frac{1}{\mu_{12}R^2}+\frac{1}{\mu_2 r_2^2},$$

$$\frac{1}{I_6(R,r_1,r_2,\theta_1,\theta_2)}=\left(\frac{1}{\mu_{12}R^2}+\frac{1}{\mu_1 r_1^2}\right)\frac{1}{\sin\theta_1^2} +\left(\frac{1}{\mu_{12}R^2}+\frac{1}{\mu_2 r_2^2}\right)\frac{1}{\sin\theta_2^2}.$$

Instead of solving the eigenvalue problem $H|\Psi\rangle=E|\Psi\rangle$ we make a transformation $\Psi(r_1,r_2,\theta_1,\theta_2,R,\phi)\Rightarrow(1/r_1r_2R)\Phi(r_1,r_2,\theta_1,\theta_2,R,\phi)$, and solve the problem $H'|\Phi\rangle=E|\Phi\rangle$, where H' is as H except for the term $T1+T2+T3$. The stretching kinetic energy parts are given for the modified problem as follows:

$$T1+T2+T3=-\frac{1}{2}\,\frac{1}{\mu_{12}}\,\frac{\partial^2}{\partial R^2}-\frac{1}{2}\,\frac{1}{\mu_1}\,\frac{\partial^2}{\partial r_1^2}-\frac{1}{2}\,\frac{1}{\mu_2}\,\frac{\partial^2}{\partial r_2^2}. \tag{3}$$

In the relevant energy region the molecular symmetry group for HOOH is $G4$.[13] It is also easy to see from the form of the Hamiltonian that the Hamiltonian is symmetric under transformations

$$H(r_1,r_2,\theta_1,\theta_2,R,2\pi-\phi)=H(r_1,r_2,\theta_1,\theta_2,R,\phi)$$

$$H(r_1,r_2,\theta_1,\theta_2,R,\phi)=H(r_2,r_1,\theta_2,\theta_1,R,\phi).$$

The Jacobi Hamiltonian enables an easy exploitation of the ϕ symmetry. The $r-\theta$ symmetry is not as easy to exploit because of the mixing of the coordinates.

B. Discretization of the kinetic energy operators

In the discrete variable representation (DVR)[2] we approximate the potential operator by its values at discrete points

$$V_{\alpha\beta}^{\text{DVR}}\equiv V(x_\alpha)\,\delta_{\alpha\beta}. \tag{4}$$

By using N classical orthogonal polynomials with appropriate weights and Gaussian quadrature points (i.e., zero points of the orthogonal polynomial ϕ_{N+1}) the DVR is isomorphic to a finite basis representation in which integrations

are carried out by using the Gaussian quadrature in question. The unitary transformations between the function bases and the point bases are given in terms of the orthogonal polynomials ϕ as

$$U_{i\alpha} \equiv \phi_i(x_\alpha)\omega_\alpha^{1/2}, \tag{5}$$

in which $\omega_\alpha^{1/2}$ is the weight associated with a Gaussian point x_α. By using these orthogonal transformations we are able to map global differential operators from function bases to point bases. (Global differential operators are more accurate than local differential operators.)[14,15]

We should note, that because of the diagonal approximation of the potential operator, DVR representations only approximate analytically calculated function basis representations. The accuracy of this approximation has, however, proved to be good.

1. "Regular" DVR operators

For radial coordinates R, r_1, and r_2 we use sine-functions. In this case Gaussian points are equally spaced with unit weights. The unitary transformation matrix is given as[16]

$$U_{\alpha n} = \langle x_\alpha | \sin\ K_n \rangle = \sqrt{\frac{2}{(N+1)\Delta x}} \sin \frac{n\pi}{(N+1)\Delta x} \times (x_\alpha - x_0), \tag{6}$$

where

$$K_n = \frac{n\pi}{(N+1)\Delta x} \quad n=1,..,N,$$

$$x_\alpha = x_0 + \alpha \Delta x \quad \alpha = 1,..,N,$$

$$\Delta x = \frac{1}{\eta\sqrt{2\mu E_{\max}}}.$$

The maximum momentum that can be presented in this grid is $\pi/\Delta x$. In $\Delta x\ E_{\max}$ is the cutoff energy and η is a parameter typically of the order of 1–2.[17]

The kinetic energy operator in the point basis is easily expressed as

$$T_{\alpha\beta} = \frac{1}{2\mu} \sum_n U_{\alpha n} K_n^2 U_{\beta n}^T. \tag{7}$$

For θ_1 and θ_2 we use Legendre polynomials. The unitary transformation matrix is given as

$$U_{\alpha l} = \sqrt{\omega_\alpha} P_l(\cos\ \theta_\alpha), \tag{8}$$

where $l = 0,..L-1$ and $\alpha = 1,..,L$.

In the point basis we have

$$T = \frac{1}{2} U \Lambda U^T$$
$$\Lambda_{ll'} = l(l+1)\delta_{ll'}. \tag{9}$$

For the torsion coordinate we use a Fourier basis

$$\Phi_n(\phi_j) = \frac{e^{in\phi_j}}{\sqrt{2\pi}} \quad n = -N,..,N,$$
$$\phi_j = j\,\frac{2\pi}{2N+1} \quad j = 1,..,2N+1. \tag{10}$$

In the point basis we have for T_ϕ [i.e. for $-(1/2)(\partial^2/\partial\phi^2)$] matrix elements[18,19]

$$T_{nn'} = \begin{cases} (-1)^{n-n'}\,\frac{1}{2}\,\frac{N(N+1)}{3} & n = n' \\ (-1)^{n-n'}\,\frac{1}{2}\,\frac{\cos\left(\frac{\pi(n-n')}{2N+1}\right)}{2\,\sin^2\left(\frac{\pi(n-n')}{2N+1}\right)} & n \neq n' \end{cases}. \tag{11}$$

The first order derivates are calculated in a similar way.

In the Legendre function basis we have

$$\left\langle P_m \left| \frac{\partial}{\partial\theta} \right| P_n \right\rangle = -\left\langle P_m(x)\,\frac{n}{\sqrt{1-x^2}}\,P_{n-1}(x) \right\rangle + \left\langle P_m(x)\,\frac{nx}{\sqrt{1-x^2}}\,P_n(x) \right\rangle$$
$$= -\sum_{j=1} \omega_j P_m(x_j)\,\frac{n}{\sqrt{1-x_j^2}}\,P_{n-1}(x_j) + \sum_{j=1} \omega_j P_m(x_j)\,\frac{nx_j}{\sqrt{1-x_j^2}}\,P_n(x_j). \tag{12}$$

With the help of the transformation matrices this can be rewritten as

$$\left\langle P_m \left| \frac{\partial}{\partial\theta} \right| P_n \right\rangle = -\sum_{j=1} U_{j,m}\,\frac{n}{\sqrt{1-x_j^2}}\,U_{j,n-1} + \sum_{j=1} U_{j,m}\,\frac{nx_j}{\sqrt{1-x_j^2}}\,U_{j,n}.$$

In the point basis we have

$$\left(\frac{\partial}{\partial\theta}\right)_{\alpha\beta} = \sum_{m,n} U_{\alpha m} \langle P_m | \frac{\partial}{\partial\theta} | P_n \rangle U_{\beta n}. \tag{13}$$

Similarly, for the Fourier points we can derive a point basis result

$$\left(\frac{\partial}{\partial\phi}\right)_{nn'} = \begin{cases} 0 & n = n' \\ (-1)^{n-n'}\,\frac{1}{2\,\sin\left(\frac{\pi(n-n')}{2N+1}\right)} & n \neq n'. \end{cases} \tag{14}$$

2. Symmetry adapted operators

For ϕ operators it is easy to build symmetry adapted operators.[20,21] We form symmetric and antisymmetric points from the Fourier points. Symmetric DVR points are

$$|\phi_j^s\rangle = \frac{1}{\sqrt{2}}(|\phi_j\rangle + |\phi_{2N+1-j}\rangle), \quad j=1,..N$$
$$|\phi_{N+1}^s\rangle = |\phi_{2N+1}\rangle, \quad j=N+1, \tag{15}$$

and antisymmetric DVR points are given as

$$|\phi_j^{as}\rangle = \frac{1}{\sqrt{2}}(|\phi_j\rangle - |\phi_{2N+1-j}\rangle), \quad j=1,..,N. \tag{16}$$

Odd FBR (finite basis representation) operators, which are calculated in a sine basis, are mapped to the antisymmetric DVR by unitary matrices

$$U_{jn}^{as} = \langle \phi_j^{as} | \sin n\phi \rangle, \quad j,n=1,..,N. \tag{17}$$

Even FBR operators are calculated in a cosine basis, and unitary transformation matrices are as follows:

$$U_{jn}^{s} = \langle \phi_j^{s} | \cos n\phi \rangle, \quad j,n=0,..,N. \tag{18}$$

Both in the sine and cosine function bases we calculate operators

$$\left(\frac{\partial^2}{\partial\phi^2}\right)_{nm} = -n^2\delta_{n,m} \tag{19}$$

and

$$\left(\sin\phi\,\frac{\partial}{\partial\phi}\right)_{nm} = -\frac{m}{4}(\delta_{m,n+1} - \delta_{n,m+1}), \tag{20}$$

in which $n, m=1,..,N$. In the cosine basis we also have

$$\left(\sin\phi\,\frac{\partial}{\partial\phi}\right)_{01} = -\frac{1}{2}. \tag{21}$$

It should be noted that in the symmetry adapted DVR the antisymmetricity of both $\sin\phi$ and $\partial/\partial\phi$ requires the calculation of the matrix elements of the product $\sin\phi(\partial/\partial\phi)$.

III. ADIABATIC PSEUDOSPECTRAL REPRESENTATION

A. An adiabatic basis set

In this section we explicitly explain the construction of an adiabatic basis set. The set is constructed sequentially, and in each step, states that do not satisfy energy and quantum number criteria are thrown away. By using this sequential truncation method we are able to build a basis set which spans only the relevant part of the space. The eigenvalues of the total Hamiltonian are computed by using this compact basis set.

We first fix $r_2 = r_{2_i}$, $\theta_1 = \theta_{1_j}$, $\theta_2 = \theta_{2_k}$, $R=R_l$ and $\phi=\phi_m$, and solve an eigenvalue problem

$$(T2+V)\,\eta_{a,i,j,k,l,m}(r_1;i,j,k,l,m) = E_{a,i,j,k,l,m}\,\eta_{a,i,j,k,l,m}(r_1;i,j,k,l,m). \tag{22}$$

Explicitly the $T2+V$ Hamiltonian is diagonalized by using a trial function

$$\eta_{a,i,j,k,l,m}(r_1;i,j,k,l,m) = \sum_{h=1}^{N_{r_1}} q_h^a \left(\begin{array}{c}\vdots\\0\\1^{h^{\text{th}}}\\0\\\vdots\end{array}\right)_{r_1} \left(\begin{array}{c}\vdots\\0\\1^{i^{\text{th}}}\\0\\\vdots\end{array}\right)_{r_2} \left(\begin{array}{c}\vdots\\0\\1^{j^{\text{th}}}\\0\\\vdots\end{array}\right)_{\theta_1} \times \left(\begin{array}{c}\vdots\\0\\1^{k^{\text{th}}}\\0\\\vdots\end{array}\right)_{\theta_2} \left(\begin{array}{c}\vdots\\0\\1^{l^{\text{th}}}\\0\\\vdots\end{array}\right)_{R} \left(\begin{array}{c}\vdots\\0\\1^{m^{\text{th}}}\\0\\\vdots\end{array}\right)_{\phi}, \tag{23}$$

where N_{r_1} is the number of r_1 points. In the points in which V exceeds a cutoff value, a large value $V_{\max}$ is used instead. Diagonalizations produce N_{r_1} eigenfunctions $\eta_{a,i,j,k,l,m}$ (i.e., coefficients q_h^a) and eigenvalues $E_{a,i,j,k,l,m}$ for every fixed point ($r_2 = r_{2_i}$, $\theta_1 = \theta_{1_j}$, $\theta_2 = \theta_{2_k}$, $R=R_l$, $\phi=\phi_m$). Only states which satisfy an energy criterion $E_{\text{state}} < E_{\text{co}}$ and a quantum number criterion $a < N_{\text{co}}$ are saved.

In the next stage we include T_3 in the Hamiltonian and calculate the matrix elements of T_2+T_3+V for every fixed quantum number point combination (a, $\theta_1 = \theta_{1_j}$, $\theta_2 = \theta_{2_k}$, $R=R_l$, $\phi=\phi_m$) by using a trial function

$$\psi_{a,b,j,k,l,m}(r_1,r_2;j,k,l,m) = \sum_{i=1}^{N_{r_2}} p_i^b\,\eta_{a,i,j,k,l,m}(r_1;i,j,k,l,m), \tag{24}$$

where N_{r_2} is the number of r_2 points. In the diagonalization the adiabatic energies $E_{a,i,j,k,l,m}$ form a potential energy surface, and the kinetic energy operator $T3$ is replaced by $T3^*$

$$T3^*_{i_x i_y} = \langle \eta_{a,i_x,j,k,l,m} | \eta_{a,i_y,j,k,l,m} \rangle T3_{i_x i_y}. \tag{25}$$

Explicitly we diagonalize matrices

$$E_{a,i_x,j,k,l,m}\delta_{i_x i_y} + T3^*_{i_x i_y}. \tag{26}$$

Diagonalizations produce adiabatic states $\psi_{a,b,j,k,l,m}$ and energies $E_{a,b,j,k,l,m}$. Again, only states satisfying energy and quantum number criteria are saved.

Next we include $(1/I_4)T_4$ in the Hamiltonian and diagonalize $T2+T3+(1/I_4)T_4+V$ for every fixed quantum number point combination (a, b, $\theta_2 = \theta_{2_k}$, $R=R_l$, $\phi=\phi_m$) by using a trial function

$$\chi_{a,b,c,k,l,m}(r_1,r_2,\theta_1;k,l,m) = \sum_{j=1}^{N_{\theta_1}} s_j^c\,\psi_{a,b,j,k,l,m}(r_1,r_2;j,k,l,m), \tag{27}$$

where N_{θ_1} is the number of θ_1 points.

Again, before diagonalizing, we compute inner products

$$\frac{1}{I_4}T4^*_{j_x j_y} = \langle \psi_{a,b,j_x,k,l,m} | \frac{1}{I_4} | \psi_{a,b,j_y,k,l,m} \rangle T4_{j_x j_y}. \tag{28}$$

We diagonalize

$$E_{a,b,j_x,k,l,m}\delta_{j_xj_y}+\frac{1}{I_4}\,T4^*_{j_xj_y}, \tag{29}$$

and get states $\chi_{a,b,c,k,l,m}$ with energies $E_{a,b,c,k,l,m}$. As before only states satisfying energy and quantum number criteria are saved.

We proceed in a similar fashion, fix the quantum number point combination $(a,b,c,\ R=R_l,\ \phi=\phi_m)$, and include $(1/I_5)T_5$ in the Hamiltonian H. Diagonalizations are carried out by using a trial function

$$\xi_{a,b,c,d,l,m}(r_1,r_2,\theta_1,\theta_2;l,m)=\sum_{k=1}^{N_{\theta_2}} t_k^d\chi_{a,b,c,k,l,m}(r_1,r_2,\theta_1;k,l,m), \tag{30}$$

where N_{θ_2} is the number of θ_2 points.

Before diagonalizing we have to calculate inner products

$$\langle\chi_{a,b,c,k_x,l,m}|\frac{1}{I_5}|\chi_{a,b,c,k_y,l,m}\rangle T5_{k_xk_y}. \tag{31}$$

Diagonalizations produce states $\xi_{a,b,c,d,l,m}$ with energies $E_{a,b,c,d,l,m}$. These energies serve as potential energy surfaces in the next step of the computation.

In the next stage we diagonalize $H=T2+T3+(1/I_4)T4+(1/I_5)T5+T1+V$ for every quantum number point combination $(a,b,c,d,\ \phi=\phi_m)$ by using the following trial function:

$$\zeta_{a,b,c,d,e,m}(r_1,r_2,\theta_1,\theta_2,R;m)=\sum_{l=1}^{N_R} u_l^e\xi_{a,b,c,d,l,m}(r_1,r_2,\theta_1,\theta_2;l,m), \tag{32}$$

where N_R is the number of R points.

Inner products have to be calculated as earlier:

$$T1^*_{l_xl_y}=\langle\xi_{a,b,c,d,l_x,m}|\xi_{a,b,c,d,l_y,m}\rangle T1_{l_xl_y}. \tag{33}$$

Explicitly we have to diagonalize matrices

$$E_{a,b,c,d,l_x,m}\delta_{l_xl_y}+T1^*_{l_xl_y}. \tag{34}$$

Diagonalizations produce eigenfunctions $\zeta_{a,b,c,d,e,m}$ and energies $E_{a,b,c,d,e,m}$.

In the final stage we fix quantum numbers (a,b,c,d,e), include $(1/I_6)T6$ in the Hamiltonian, and solve an eigenvalue problem

$$\left(T1+T2+T3+\frac{1}{I_4}\,T4+\frac{1}{I_5}\,T5+\frac{1}{I_6}\,T6+V\right)\rho_{a,b,c,d,e,f}(r_1,r_2,\theta_1,\theta_2,R,\phi)=E_{a,b,c,d,e,f}\rho_{a,b,c,d,e,f}(r_1,r_2,\theta_1,\theta_2,R,\phi). \tag{35}$$

The trial function is given as

$$\rho_{a,b,c,d,e,f}(r_1,r_2,\theta_1,\theta_2,R,\phi)=\sum_{m=1}^{N_\phi} v_m^f\zeta_{a,b,c,d,e,m}(r_1,r_2,\theta_1,\theta_2,R;m), \tag{36}$$

where N_ϕ is the number of ϕ points.

As earlier we have to compute inner products

$$T6^*_{m_xm_y}=\langle\zeta_{a,b,c,d,e,m_x}|\frac{1}{I_6}|\zeta_{a,b,c,d,e,m_y}\rangle T6_{m_xm_y}. \tag{37}$$

For every quantum number combination (a,b,c,d,e) we have the following one dimensional matrix to diagonalize:

$$E_{a,b,c,d,e,m_x}\delta_{m_xm_y}+T6^*_{m_xm_y}. \tag{38}$$

Diagonalizations give us final energies $E_{a,b,c,d,e,f}$ and states $\rho_{a,b,c,d,e,f}$.

Our sequential procedure enables us to build a compact basis set and reduce the number of functions significantly, roughly by a factor of 10^2 to 10^3. In our procedure we are also able to tailor the basis set by imposing different energy and quantum number criteria in each of the steps. The most significant reduction in the number of states is achieved already in the first step by disregarding high energy points of the ground state electronic potential energy surface. In spite of criticism against this procedure in Ref. 9, the procedure has been proved to be successful, e.g., in Refs. 7 and 22. In practical computations we used a modified energy cutoff criterion in the first step of the construction of the adiabatic basis set. In one dimensional diagonalizations we replaced only energies at points with $V>V_{\rm co}^{\rm high}$ by $V_{\rm large}$. In Lanczos diagonalization we, however, included only points with $V<V_{\rm co}^{\rm low}$. The purpose of this two level energy cutoff criterion was to have more correct tails in wave functions and to have more accurate adiabatic energies $E_{a,i,j,k,l,m}$. In each other stage of our procedure we used a high energy $E_{\rm large}$ for the potential energy, if the state had been thrown away in the previous step of the computation.

It should be noted that our adiabatic basis set is not unique, and we could e.g. have included the coupling terms $TC1$, $TC2$, $TC3$, and $TC4$ in the construction of the adiabatic basis set. For example, the term

$$TC2=\frac{1}{\mu_{12}R^2}\left(-\sin\,\phi\,\cot\,\theta_2\,\frac{\partial^2}{\partial\theta_1\partial\phi}\right)$$

could have easily been included, e.g., in the definition of the θ_1 dependent part of the adiabatic functions. [Please see Eqs. (27) and (28).] After diagonalizing $T2+T3+V$ we could not only have included $(1/I_4)T_4$ but also $TC2$ in the Hamiltonian. In practice we would just have had to compute extra terms

$$\langle\psi_{a,b,j_x,k,l,m}|-\left(\frac{1}{\mu_{12}R^2}\,\sin\,\phi\,\cot\,\theta_2\,\frac{\partial^2}{\partial\theta_1\partial\phi}\right)|\psi_{a,b,j_y,k,l,m}\rangle. \tag{39}$$

In the previous equation we have fixed ϕ and θ_2, and therefore different ψs are only coupled by

$$\frac{1}{\mu_{12}R^2}\,\frac{\partial}{\partial\theta_1}.$$

B. The least squares matrices

In this section we form the least squares matrices and their inverses from the adiabatic vectors computed in the sequential adiabatic states construction procedure described in the previous section. The least squares matrices and their inverses are used to map wave functions between the physical space and the spectral space.

For each of the blocks i,j,k,l,m ($r_2 = r_{2_i}$, $\theta_1 = \theta_{1_j}$, $\theta_2 = \theta_{2_k}$, $R = R_l$ and $\phi = \phi_m$) we have least squares matrices R and their inverses G

$$(R_{r_1}^{i,j,k,l,m})_{a,p} = (\eta_{a,i,j,k,l,m})_p^T, \quad a = 1,2,..,N_{i,j,k,l,m} \quad p = 1,2,..,N_{r_1}$$
$$G = (RR^T)^{-1}R^T. \tag{40}$$

In the previous equation N_{r_1} and $N_{i,j,k,l,m}$ refer to the total number of r_1 points and the total number of saved vectors in the i,j,k,l,m block, respectively.

With similar notations as in the previous equation the rest of the least squares matrices are given as follows:

$$(R_{r_2}^{a,j,k,l,m})_{b,p} = (\psi'_{a,b,j,k,l,m})_p^T, \quad b = 1,2,..,N_{a,j,k,l,m} \quad p = 1,2,..,N_{r_2}, \tag{41}$$

$$(R_{\theta_1}^{a,b,k,l,m})_{c,p} = (\chi'_{a,b,c,k,l,m})_p^T, \quad c = 1,2,..,N_{a,b,k,l,m} \quad p = 1,2,..,N_{\theta_1}, \tag{42}$$

$$(R_{\theta_2}^{a,b,c,l,m})_{d,p} = (\xi'_{a,b,c,d,l,m})_p^T, \quad d = 1,2,..,N_{a,b,c,l,m} \quad p = 1,2,..,N_{\theta_2}, \tag{43}$$

$$(R_R^{a,b,c,d,m})_{e,p} = (\zeta'_{a,b,c,d,e,m})_p^T, \quad e = 1,2,..,N_{a,b,c,d,m} \quad p = 1,2,..,N_R, \tag{44}$$

and

$$(R_\phi^{a,b,c,d,e})_{f,p} = (\rho'_{a,b,c,d,e,f})_p^T, \quad f = 1,2,..,N_{a,b,c,d,e} \quad p = 1,2,..,N_\phi, \tag{45}$$

where the primed functions refer to the *coefficients* in the respective functions [see Eqs. (24), (27), (30), (32), and (36)].

Naturally the inverse matrices are built from the appropriate R matrices as earlier, i.e., $G = (RR^T)^{-1}R^T$.

C. A single operation with the Hamiltonian

The most general spectral space wavefunction is expressed as

$$\Psi = \sum_{a,b,c,d,e,f} C_{abcdef}\rho_{a,b,c,d,e,f}, \tag{46}$$

where Cs are spectral coefficients. The wave function is easily transformed from the spectral space to the physical space by using least squares matrices R defined in the previous section. Mappings are performed sequentially, i.e., we first sum over f and represent the wave function in a mixed spectral physical representation. After f summations we carry out e, d, c, b, and a summations.

In each step the wave function is represented in a totally compressed form. The use of a compressed representation reduces memory requirements significantly. For example, in the largest form, i.e., in the physical space, the wave function has in the sparse form $N_\phi N_{\theta_2} N_{\theta_2} N_{r_2} N_{r_1} N_R$ components. On the other hand, in the compressed form we only store wave function components which are nonzero—typically this means a reduction of the number of points by 90%–99%.

Once the wave function is expressed in the physical space we can easily act with the Hamiltonian H. Since we are in the point basis the potential operator is diagonal and we could simply act with it by multiplying the wave function by V_{point} in each of the space points. A more efficient way of operating with V (and $T2$) is easy to achieve by recognizing that the eigenfunctions of $V+T2$ are used to expand the wave function on the physical grid. Thus instead of operating separately with V and $T2$, we can operate with $V+T2$ in a mixed spectral physical space. Let the wave function Ψ to have a mixed representation of the form

$$\Psi(r_1,i,j,k,l,m) = \sum_a D_{a,i,j,k,l,m}\eta_{a,i,j,k,l,m}(r_1, r_{2_i}, \theta_{1_j}, \theta_{2_k}, R_l, \phi_m). \tag{47}$$

Once the wave function is spectral in r_1 and physical in other coordinates we simply have

$$V+T2|\Psi(r_1,i,j,k,l,m)\rangle = \sum_a E_{a,i,j,k,l,m}D_{a,i,j,k,l,m} \times \eta_{a,i,j,k,l,m}(r_1; r_{2_i}, \theta_{1_j}, \theta_{2_k}, R_l, \phi_m), \tag{48}$$

where $E_{a,i,j,k,l,m}$s are adiabatic energies from the first step of the sequential adiabatic basis set construction procedure. The application of the rest of the kinetic energy operators is also straightforward. When acting, e.g., with T_ϕ we first fix R, r_1, r_2, θ_1, and θ_2, "pick up" the relevant points from the compressed wave function to an uncompressed vector of the length of N_ϕ and perform a multiplication

$$\hat{T}_\phi\Phi(\phi_\alpha, R_i, r_{1_j}, r_{2_k}, \theta_{1_l}, \theta_{2_m}) = \sum_\beta T_{\phi_{\alpha\beta}}\Phi(\phi_\beta, R_i, r_{1_j}, r_{2_k}, \theta_{1_l}, \theta_{2_m}). \tag{49}$$

After acting with the kinetic energy operator T_ϕ we multiply the wave function by the relevant part of $(1/I_\phi)$ and compress the resulting vector. Once we have acted with all of the kinetic energy operators we map the wave function back to the spectral space by using the inverse least squares matrices G.

It is good to notice that both in the least squares mappings and the application by the Hamiltonian the use of several 1 dimensional matrices is more efficient than the use of 1 or many larger dimensional matrices. This is easy to see by assuming M coordinates each having N components. On the

one hand, a single matrix containing all of the coordinates would be of size $N^M * N^M$. This means we would have to perform N^{2M} vector–vector multiplications each time we apply with the matrix. On the other hand, with M separate matrices of size $N*N$ we would have $N*N*N^M/N$ (N^{M-1} N component vectors in the full length vector) vector–vector multiplications for each coordinate; i.e., totally we would have $M*N^{M+1}$ vector–vector multiplications to carry out. A further point to notice is that data compression enables one to reduce significantly computational effort throughout the computation.

D. The Lanczos diagonalization

We diagonalize our Hamiltonian in a space spanned by the adiabatic vectors. First we tridiagonalize the Hamiltonian by using the Lanczos algorithm. After tridiagonalization eigenvalues are obtained by the modified QL factorization.[23]

The Lanczos algorithm builds an orthogonal basis in the Krylov space $|\Psi\rangle$, $H|\Psi\rangle,\ldots,H^n|\Psi\rangle$. (The fact that orthogonality of Lanczos vectors is lost in finite precision does not reduce the reliability of eigenvalue calculations.[3,24]) In this space the Hamiltonian is tridiagonal. The Lanczos recursion step is given as

$$\beta_{n+1}|\Psi_{n+1}\rangle = H|\Psi_n\rangle - \alpha_n|\Psi_n\rangle - \beta_n|\Psi_{n-1}\rangle. \tag{50}$$

In the previous equation $\alpha_n = \langle\Psi_n|H|\Psi_n\rangle$ and $\beta_n = \langle\Psi_{n-1}|H|\Psi_n\rangle$, i.e., in the tridiagonal Hamiltonian αs are the diagonal elements and βs are the off-diagonal elements.

The Lanczos tridiagonalization has several advantages as compared to the QR diagonalization. The Lanczos algorithm easily enables the use of an operator form of the Hamiltonian. Instead of having to store an $N*N$ DVR Hamiltonian matrix we only have to store a (small) number of small kinetic energy operator matrices and a small number of basis functions. Due to our recursive definition of adiabatic collocation functions and inverse least squares matrices the storage requirement is practically N_s*N, where N_s is a small number of the order of 10 and N is the number of points in a vector. The CPU requirements are also smaller than in a QR diagonalization. In the Lanczos–QL procedure it is easy to achieve a scaling between N and N^2 as compared to that of N^3 in the QR diagonalization.

A factor that reduces the number of required Lanczos iterations is the use of a basis set which spans a narrow energy range. This comes from the fact that the rate of convergence of the Lanczos algorithm depends on the spread in energies. Thus the use of a tailored adiabatic basis set not only reduces the number of required basis functions but it also reduces the iteration time.

An efficient way to reduce computational effort is to take into account the symmetries of the Hamiltonian. With the Jacobi Hamiltonian it is easy to build a ϕ symmetry adapted adiabatic basis set. The splitting of the problem to ϕ symmetric and ϕ antisymmetric computations reduces not only the sizes of the adiabatic spaces but also the spectral densities, and thereby also the computational time. The use of a symmetry adapted adiabatic basis set guarantees that our computations stay within a symmetry block of the Hamiltonian. It is more difficult to build a basis set with $r-\theta$ symmetries. In principle the initialization of the initial vector to a particular $r-\theta$ symmetry block should guarantee that the computation stays within a symmetry block of the Hamiltonian even without a symmetry adapted basis set. In practise, however, numerical errors cause leakage from the original symmetry block to other symmetry blocks.

TABLE I. Low-lying HOOH vibrational levels.

n	a	b	c	d	e
1	13.22	13.22	13.2	*S-AS*	$0\mu_4$
2	258.46	258.46	258.5	*S-S*	$1\nu_4$
3	380.45	380.45	380.8	*S-AS*	$1\mu_4$
4	564.73	564.73	565.0	*S-S*	$2\nu_4$
5	735.02	735.01	735.2	*S-AS*	$2\mu_4$
6	847.46	847.41	847.4	*S-S*	ν_3
7	882.83	882.79	882.5	*S-AS*	ν_3
8	1270.82	1270.81	1273.8	*AS-S*	ν_6
9	1284.64	1284.65	1287.2	*AS-AS*	ν_6
10	1382.01	1381.91	1379.2	*S-S*	ν_2
11	1392.12	1392.05	1389.7	*S-AS*	ν_2
12	2629.26	2629.03	2630.0	*AS-S*	$\nu_2+\nu_6$
13	2639.88	2639.80	2640.7	*AS-AS*	$\nu_2+\nu_6$
14	3602.14	3601.74	3605.3	*S-S*	ν_1
15	3603.38	3603.00	3606.9	*AS-S*	ν_5
16	3615.26	3614.47	3618.0	*S-AS*	ν_1
17	3616.25	3615.99	3619.8	*AS-AS*	ν_5
18	4445.61		4449.0	*AS-S*	$\nu_3+\nu_5$
19	4480.08		4483.4	*AS-AS*	$\nu_3+\nu_5$
20	4861.24		4867.5	*AS-S*	$\nu_1+\nu_6$
21	4874.86		4880.0	*AS-AS*	$\nu_1+\nu_6$
22	4972.60		4973.1	*AS-S*	$\nu_2+\nu_5$
23	4982.28		4983.2	*AS-AS*	$\nu_2+\nu_5$

[a]Results from Ref. 8.
[b]Results from Ref. 9.
[c]Results from our computations.
[d]Symmetry labels 1st $r-\theta$, 2nd ϕ.
[e]Normal mode labels. Results a and b from the ground state of 5692.2 wave numbers. Results c from the ground state of 5692.9 wave numbers.

IV. RESULTS

In our computations we used the same potential energy surface as was used in Refs. 8 and 9. The potential energy surface is the V_g surface from Ref. 12 and is ''a good representation of the potential in the region of the equilibrium geometry.'' The inaccuracy of the potential energy surface far from the equilibrium geometry complicated both the determination of an appropriate potential energy box in which computations were to be performed and the design of the physical grid.

In our computations we used a ϕ-symmetry adapted basis set. We initialized the computations by using normal mode initial vectors computed by ASYM 20 program.[25,26] In the normal mode description the first excited state in the normal coordinate q is proportional to $q|\Psi_0\rangle$, in which $|\Psi_0\rangle$ is the ground state. The ground state was computed by the Conjugate Gradient Method.[27] By using a normal mode as an initial vector, Lanczos procedure produces a strong residue to the normal mode in question. The normal mode labels assigned based on strong residues are (see Table I) $\nu 1$ O–H

TABLE II. CPU time requirements as a function of V_{co}^{low}.

n	a	b	c	d
1	18 000	233 551	4 088	4.26
2	20 000	313 611	7 450	5.49
3	22 000	406 852	12 509	6.93
4	24 000	511 168	12 489	8.02
5	25 000	567 508	12 489	9.58
6	28 000	745 050	12 487	10.56

[a]V_{co}^{low} from the bottom of the potential well.
[b]Number of symmetric points.
[c]Number of adiabatic vectors.
[d]CPU seconds/Lanczos iteration. In Eqs. (3)–(6) $E_{co}=22\,000$ wave numbers. In Eqs. (1) and (2) $E_{co}=V_{co}^{low}$ wave numbers.

symmetric stretch, $\nu 2$ O–O–H symmetric bend, $\nu 3$ O–O stretch, $\nu 4$ and $\mu 4$ torsion, $\nu 5$ O–H antisymmetric stretch and $\nu 6$ O–O–H antisymmetric bend. Proper initialization enables an easy identification not only of the lowest levels but also of the excited states. In this paper we, however, present results only for the few selected lowest energy states.

The computations were carried out on an IBM 580 work station. We used 21 points for O–O–H bending coordinates, 10 points for the symmetric torsion, 9 points for the antisymmetric torsion, 8 points for O–H stretches, and 13 points for the O–O stretch. As potential energy cutoffs we used $V_{co}^{high}=28\,000$ wave numbers (for one dimensional diagonalizations) and $V_{co}^{low}=24\,000$ wave numbers (for the Lanczos diagonalization). The energy cutoff value for the other than the first one-dimensional diagonalizations in the adiabatic basis set construction procedure was $E_{co}=22\,000$ wave numbers. As quantum number cutoffs four was used for the first and the second O–H stretch and ten for all the other vectors. The total number of symmetric and antisymmetric points used in Lanczos iteration were, respectively, 511 168 and 483 755. The lowering of V_{co}^{low} to 20 000 wave numbers (313 611 symmetric points and 297 788 antisymmetric points) changed levels below 3600 wave numbers less than 0.5 wave numbers, and levels above 3600 1–2 wave numbers. The results presented in Table I are converged with respect to the number of points and energy cutoffs. The convergence in the Lanczos sense, i.e., the residue does not change more than 10% and the energy does not change more than 0.1 wave numbers as compared to the numbers 50 iterations earlier, occurred for states up to 2640 wave numbers during the first 100 iterations and for the highest states roughly within 300–500 iterations. Convergence as a function of iteration number is presented in Table III. The ''oscillation'' of the higher levels as seen in Table III is caused by a property of the Lanczos algorithm: Dense parts of a spectrum are difficult for the Lanczos algorithm and the iteration converges most quickly in the sparse parts of the spectrum. In Table IV we used as an initial vector a weighted sum of the normal modes used in Tables I and III. The convergence is presented as in Table III. The minor discrepancies between the single mode (Table III) and multimode (Table IV) results can be explained by weak intensities of some of the lines and a much denser spectrum in the multimode case. Levels 14 and 15, and 16 and 17 merged because of their close proximity. As explained earlier this problem could be reduced by exploiting a $r-\theta$ symmetry adapted

TABLE III. Convergence of levels as a function of the number of iterations. Levels are the same as in Table I ($V_{co}^{low}=24\,000$ wave numbers). In the table only the changed digits are presented. The last column gives final numbers). U means that the level was not identifiable. R means that the residue criterion of the residue not changing more than 10% as compared to the situation 50 recursions earlier was satisfied. Single mode initial vector.

n	50	100	150	200	250	300	350	400	450	500	550	600
1	13.2	R										13.2
2	258.5	R										258.5
3	380.8	R										380.8
4	565.0	R										565.0
5	735.2	R										735.2
6	847.0	.4R										847.4
7	882.9	.5R										882.5
8	1273.8	R										1273.8
9	1287.2	R										1287.2
10	1379.2	R										1379.2
11	U	1389.7	R									1389.7
12	2630.2	.0R										2630.0
13	2642.0	0.7R										2640.7
14	3605.1	.1R	.3	.3	.5	.3						3605.3
15	3606.9	7.1R	6.9					.6	.9		.6	3606.9
16	3616.9	7.8R	6.9	5.4	8.0							3618.0
17	3619.1	.6R	8.9	9.8								3619.8
18	4449.2	50.3R	47.2	8.8	.5	.8	9.0					4449.0
19	U	4483.9	.2R	.4	.2	.4		.7		.4		4483.4
20	4868.0	6.9R	7.5									4867.5
21	4881.6	79.6R	80.2		.5	.9	.5		79.8		80.0	4880.0
22	U	4972.4	.6R	3.3	.1							4973.1
23	U	4980.5	3.4R	.2								4983.2

TABLE IV. Convergence of levels as a function of the number of iterations. Levels are the same as in Table I (V_{co}^{low}=24 000 wave numbers. In the table only the changed digits are presented. The last column gives final numbers. U means that the level was not identifiable. * means that the level did split. An intensity weighted average of the nearest levels is given. Multimode initial vector.

n	50	100	150	200	250	300	350	400	450	500	550	600
1	13.4											13.4
2	259.0											259.0
3	381.2											381.2
4	563.6	4.5										564.5
5	734.8	5.0										735.0
6	842.8	6.5										846.5
7	881.4	2.7										882.7
8	1273.8											1273.8
9	1287.7	.2										1287.2
10	1391.7	79.0										1379.0
11	1413.0	389.5										1389.5
12	2632.2	0.4	.0									2630.0
13	2650.8	37.4	41.6	0.7	.9							2640.7
14	3606.6	.0	4.7	6.2	.4	.2		.0	5.8	6.2		3606.2
17	3618.7	.3	9.1	8.9	.7	9.4	.1					3619.4
18	4472.7	52.5	1.0*	46.6	8.1	.3		.5				4448.5
19	4490.9	84.3	.8	1.5	.0	2.4*	4.1	3.9	.2	.7		4483.7
20	4875.9	62.7	7.1	.3			.2*	.3				4867.3
21	4894.7	6.7	79.8	80.3		.5	.7	.0	.3	.5		4880.5
22	U	4930.9	79.7	8.4	3.1	.3	.5	.5*	.9	.3		4973.3
23	U	U	U	4993.7	81.9			3.0	.2			4983.4

adiabatic basis set, and thereby reducing the density of the spectrum. In Fig. 2 we present a ϕ-antisymmetric spectrum, in which residues as well as eigenvalues are calculated via the RRGM procedure.[23] The initial state for the recursion is the weighted sum of normal modes used previously. This rather dense spectrum does not describe a particular physical situation, but is used to study the convergence of the strongest lines of the spectrum. We expect that the convergence of this model with respect to line intensities is similar to that which would be observed for actual spectroscopic calculations, i.e., for SEP spectra as such as were calculated in Ref. 7. The convergence of the 22 strongest lines of the spectrum presented in Fig. 2 was studied by calculating an error number $[1-\Sigma_{i=1}^{22} I_i(\text{recursion number})/\Sigma_{i=1}^{22} I_i(4000 \text{ iterations})]$. The error number for these 22 lines, which as converged took 98% of the total intensity, is presented in Fig. 3. Whereas some of the oscillation seen in Fig. 3 is real and caused by the Lanczos algorithm, some abrupt peaks are caused by pattern recognition problems. For example, the peak seen at 3300 recursions in Fig. 3 was caused by an artificial merging of a weak line to one of the 22 lines studied. By artificial we mean that the lines were clearly distinguishable by eye, but not by the rather primitive pattern recognition algorithm. The convergence of the spectrum is for the most part very rapid. For example 1% error is achieved after a few hundred iterations and 0.1% error after roughly 1000 iterations. This property will be useful in the optimization of potential functions.

With regard to accuracy, our results are all within 6 cm^{-1} of those from Refs. 8 and 9 and within 2 cm^{-1} for the majority of cases. It is difficult to quantify at present the sources of these discrepancies: As noted earlier, several factors (e.g., convergence of the Lanczos procedure) have been

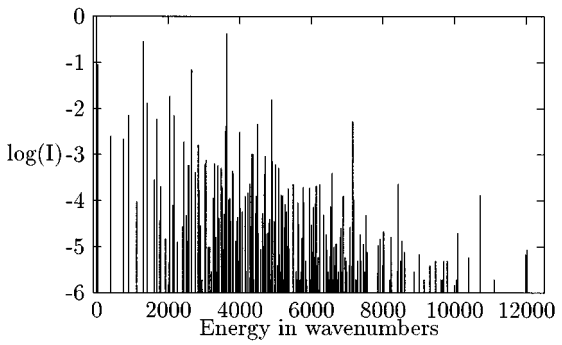

FIG. 2. Simulated antisymmetric spectrum at 4000 Lanczos recursions.

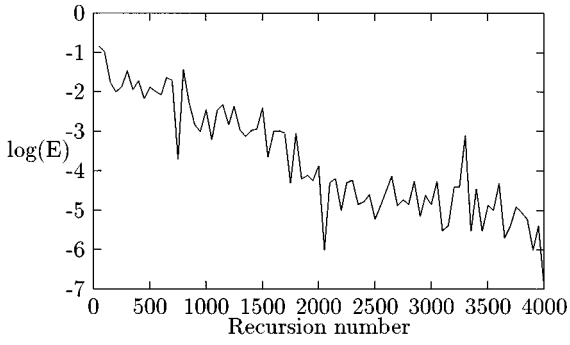

FIG. 3. Error, E, of the 22 strongest levels as a function of the iteration number.

eliminated. We intend to pursue this question in a subsequent publication.

We have made a substantial effort to make the code CPU efficient. Not taking into account the time needed to define an appropriate potential energy box, the preprocessing time is mostly consumed in the construction of the adiabatic basis set. For the case $V_{co}^{low}=24000$ wave numbers the adiabatic basis construction takes 2900 CPU seconds of which the rather slow potential energy subroutine takes 600 s. Otherwise the inner products needed to weight the point basis kinetic energy operators are the most time consuming part of the basis construction. The CPU requirements of the iterative parts of computations are presented in Table II. As expected, we have spent more time in an effort to increase the efficiency of the iterative part than the preprocessing part of the program. The most significant single factor in (iterational) computational time is the number of points in which operations with the Hamiltonian are performed. A sure way to increase the efficiency of the code would be an explicit exploitation of the $r-\theta$ symmetry of the Hamiltonian. This would, however, mean some tedious algebraic manipulation, which is not essential to the demonstration of the efficiency of the adiabatic pseudospectral method. As can be noticed, for a computation of same size, our program requires significantly less computational time than the programs used in Refs. 8 and 9. In addition to the requirement for the CPU time a factor which is of great interest is the total fast memory usage of the code. The version of the code which can handle the largest computation presented in this paper (i.e., $V_{co}^{low}=28\,000$ wave numbers) needs 200 MB of fast memory. Of these 200 MB the collocation and inverse least squares matrices consume roughly 40% and different pointers approximately 20%. The rest consists mainly of redundant work space and other auxiliary space. Most of the work space usage is directly proportional to the number of non zero wave function components, which makes the scaling of the needed memory space rather good. Significant memory could, however, be saved by a more careful design of the use of work space and a compression of the collocation and inverse least squares matrices.

V. CONCLUSION

We have demonstrated that calculations for a strongly coupled six dimensional vibrational problem can be carried out on a workstation in a modest amount of CPU time. Further improvements in the code, faster workstations, and implementation on massively parallel machines will make these applications routine over the next several years. This will make comparison with a large new subset of experimental data possible.

While the calculations here involved a single gas phase molecule, the technology developed in the present paper can be embedded in a methodology to treat large molecules or condensed phase dynamics in which a smaller subset of the degrees of freedom must be given accurate quantum mechanical treatment. The use of adiabatic functions in such cases is a natural one and will be developed further in future publications.

From the standpoint of further algorithm development, the most interesting question is whether the present methods can be extended to treat many more degrees of freedom and/or higher energies. The key to this must be the extensive use of cutoffs; for example, one should be able to cut off the basis set from below if simulating a small high energy window of the spectrum. As we have argued previously, this should be much easier with an adiabatic basis as the coupling matrix elements are orders of magnitude smaller than with a direct product basis. However, this will have to be demonstrated in practice before its utility can be assessed.

ACKNOWLEDGMENTS

This work was supported by a grant from the National Science Foundation. We thank Matthew Bramley and Tucker Carrington for sending us an H_2O_2 potential function subroutine and for communicating their work to us prior to publication.

[1] D. Gotlieb and S. Orszag, *Numerical Analysis of Spectral Methods* (SIAM, Philadelphia, 1977).
[2] J. C. Light, I. P. Hamilton, and J. V. Lill, J. Chem. Phys. **82**, 1400 (1985).
[3] J. K. Cullum and R. A. Willoughby, *Lanczos Algorithms for Large Symmetric Eigenvalue Computations* (Birkhaüser, Boston, 1985).
[4] Z. Basic and J. C. Light, J. Chem. Phys. **85**, 4594 (1986).
[5] Z. Basic and J. C. Light, J. Chem. Phys. **87**, 4008 (1987).
[6] Z. Basic and J. C. Light, Ann. Rev. Phys. Chem. **40**, 469 (1989).
[7] R. A. Friesner, J. A. Bentley, M. Menou, and C. Leforestier, J. Chem. Phys. **99**, 324 (1993).
[8] M. J. Bramley and N. C. Handy, J. Chem. Phys. **98**, 1378 (1993).
[9] M. J. Bramley and T. Carrington, Jr., J. Chem. Phys. **99**, 8519 (1993).
[10] K. Yamanouchi, N. Ikeda, S. Tsuchiya, D. M. Jonas, J. K. Lundberg, G. W. Adamson, and R. W. Field, J. Chem. Phys. **95**, 6330 (1991).
[11] X. Chapuisat, A. Belafhal, and A. Nauts, J. Mol. Spectrosc. **149**, 274 (1991).
[12] A. Willets, J. F. Gaw, N. C. Handy, and S. Carter, J. Mol. Spectrosc. **135**, 370 (1989).
[13] P. R. Bunker, *Molecular Symmetry and Spectroscopy* (Academic, Orlando, 1979).
[14] A. Solomonoff and E. Turkel, J. Comput. Phys. **81**, 239 (1989).
[15] C. Schwartz, J. Math. Phys. **26**, 411 (1985).
[16] C. Leforestier, J. Chem. Phys. **94**, 6388 (1991).
[17] R. Kosloff, in *Numerical Grid Methods and Their Application to Schrödinger's Equation*, edited by C. Cerjan, Vol. 412 (Kluwer Academic, Dordrecht, 1993).
[18] R. Meyer, J. Chem. Phys. **52**, 2053 (1969).
[19] D. T. Colbert and W. H. Miller, J. Chem. Phys. **96**, 1982 (1992).
[20] F. Le Quere and C. Leforestier, J. Chem. Phys. **94**, 1118 (1991).
[21] R. M. Whitnell and J. C. Light, J. Chem. Phys. **89**, 3674 (1988).
[22] S. E. Choi and J. C. Light, J. Chem. Phys. **92**, 2129 (1990).
[23] R. E. Wyatt and D. S. Scott, in *Mathematical Studies Series*, edited by J. K. Cullum and R. A. Willoughby, Vol. 127 (North-Holland, Amsterdam, 1986).
[24] R. E. Wyatt, Adv. Chem. Phys. **73**, 231 (1989).
[25] L. Hedberg and I. M. Mills, J. Mol. Spectrosc. **160**, 117 (1993).
[26] L. Hedberg and I. M. Mills, ASYM 20 computer program. Dept. of Chemistry Univ. of Reading, UK.
[27] W. W. Hager, *Applied Numerical Linear Algebra* (Prentice Hall, London, 1988).